

Antimicrobial and Anticancer Properties of Hydroxyapatite Nanoparticles Doped with Biogenic Zinc: A Helpful Solution for Spinach

¹Dr. S. Puvaneswari, ²S. S. Saravanakumar, ³Mr. M. Karthigeyan, ⁴Dr. M. Manichithra, ⁵Dr. C. Mabel Joshaline, ^{6*}Dr. Subbiah Rammohan Chitra

¹Assistant Professor, Department of Physics, M. S. S. Wakf Board College, Madurai, Tamilnadu, India.

²Guest Lecturer, PG and Research Department of Physics, Sethupathy Government Arts College, Ramanathapuram, Tamilnadu, India.

³Assistant Professor, Arumugam Pillai Seethai Ammal College, Tirupattur, Sivagangai District, Tamilnadu, India.

⁴Guest Lecturer, Department of Homescience, Government Arts College for Women, Sivagangai District, Tamilnadu, India.

⁵Assistant Professor, Department of Rural Development Science, Arul Anandar College, Madurai – 625514, Tamilnadu, India.

^{6*}Head and Associate Professor, Department of Physics, P K N Arts and Science College, Thirumangalam, Madurai, Tamilnadu, India.

Abstract

A stabilising ingredient called *Spinacia oleracea* L., or milk spinach, was utilised in the successful green production of zinc-hydroxyapatite nanoparticles (ZnHANPs). Through characterisation using FTIR, XRD, and SEM-EDAX, the synthesis of crystalline ZnHANPs with a mainly nanorod form and an average particle size of around 20 nm was confirmed. These nanoparticles showed great antibacterial activity against both Gram-positive and Gram-negative bacteria, in addition to having outstanding antioxidant and anticancer activities against MCF-7 human cancer cell lines. ZnHANPs' promising medicinal applications and ecologically benign production suggest that they might be a long-term solution for a variety of medical conditions.

Keywords

Spinacia oleracea L., or milk spinach, ZnHANPs, MCF-7, Antioxidant and Anticancer activities, Hydroxyapatite Nanoparticles

1. Introduction

Traditional medicine has utilised therapeutic plants since ancient times due to their exceptional inhibitory qualities [1, 2]. Nanotechnology has advanced significantly, especially in the creation of environmentally benign chemical processes and sustainable synthesis techniques. These changes have occurred in recent years. Reducing the quantity of potentially hazardous chemicals and synthetic nanoparticles (NPs) with sizes ranging from 1 to 100 nanometres is the primary objective of these methods [3]. Among the many

^{6*}Corresponding Author Mail id: jaicitra@yahoo.co.in

benefits of green synthesis are its affordability, sustainability, adaptability, biocompatibility, and potential for commercial usage. In recent years, there has been a tremendous advancement in the manufacture of hydroxyapatite (HA) nanoparticles [4, 5]. Such advancements have occurred. Many biological domains have shown great promise, such as photonics, medicine, cosmetics, and photocatalysis.

Hydroxyapatite (HA), a well studied biological material, is used in bone tissue engineering and bioactive coatings. Its biological interaction rates, however, provide some challenges. To try to solve these problems, scientists have tried combining HA with other metal ions. Zinc-doped HA has several benefits, including corrosion resistance, load-bearing capacity, anti-cancer properties, and antibacterial and antifungal properties [6]. Additionally, it enhances cell adhesion and encourages the growth of mesenchymal stem cells.

Researchers are actively investigating the potential of nanoparticle-based therapeutics to precisely target cancer cells in light of the rising concern about cancer throughout the world [7]. ZnHANPs have become a very attractive alternative due to their exceptional capacity to specifically target and eliminate cancer cells [9]. Zinc hydrazine nanoparticles (ZnHANPs) are very promising in the biomedical field because of their inherent capacity to kill cancer cells. These characteristics make them extremely advantageous for targeted chemotherapy and offer a viable strategy to fight various cancer forms. Strong evidence about the targeted killing of cancer cells and the detrimental effects of ZnHANPs on various cancer types has been presented in recent research.

Among the plant's numerous antibacterial and anticancer compounds is folic acid, which has therapeutic benefits for treating anaemia [10-13]. Spinach leaf extract is used to create green ZnHA nanoparticles, and this study is the first to demonstrate their advantageous multifunctional qualities. This new method expands the potential applications of nanoparticles in several fields, including healthcare.

2. Materials Used and Methods

2.1. Materials

Zinc nitrate ($Zn(NO_3)_2$), calcium nitrate ($Ca(NO_3)_2$), and pure diammonium hydrogen phosphate ($(NH_4)_2HPO_4$) were supplied by Merck. The leaves of *Spinacia oleracea* L. were collected from the university's property. The experiments were conducted using pure water and scientific-grade reagents.

2.2. *Spinacia oleracea* L mediated syntheses of ZnHA nanoparticles

Fresh *Spinacia oleracea* L. (milk spinach) leaves were meticulously cleansed with tap water and then distilled water (DDW) to remove impurities. The leaves were then chopped, let to air dry, and stored in the refrigerator. To make a plant extract, 20 g of dried leaves were cooked in 250 mL DDW in a water bath for 20 minutes at 100°C. The resultant mixture was cooled and filtered, and the filtrate was stored at refrigerator temperature for subsequent use. Aqueous solutions of calcium nitrate (0.9 M), zinc nitrate (0.1 M), and diammonium hydrogen phosphate ($(NH_4)_2HPO_4$) (0.6 M) were prepared. In a sonication

^{6*}Corresponding Author Mail id: jaicitra@yahoo.co.in

bath, 100 mL of diammonium hydrogen phosphate solution was dropwise combined with 100 mL of room-temperature calcium nitrate solution. The pH of the mixture was changed with liquid ammonia. The resulting solution was sonicated for two hours and then left to develop for three days. The precipitate was collected by centrifugation, washed with DDW, and dried in an oven set at 100°C for five hours. The resultant powder was crushed and stored for further analysis.

2.3 Characterization

FTIR analysis, powder X-ray diffraction, scanning electron microscopy, and transmission electron microscopy were used in the study to look at the morphology, XRD patterns, and microstructure of a sample. The Perkin-Elmer 100 spectrometer was used for FTIR analysis, while the XPERT-PRO diffractometer was used for XRD. The microstructure was examined at the nanoscale using a Titan G2 60-300 microscope.

2.4 Antioxidant Activity

The protocol described by Milar Dovic et al. [14] was followed. For the research, ZnHANPs were synthesised at different concentrations and mixed with a 0.2 M DPPH solution. The resulting mixture shifted from purple to yellow, indicating antioxidant activity. The absorbance of the solution was measured using an ultraviolet (UV)-visible spectrophotometer with an absorbance wavelength of 517 nm in order to identify changes in absorbance as DPPH dropped. Vitamin C was used as a control to determine how many ZnHANPs were needed to eliminate 50% of the DPPH radical.

$$\% \text{ Inhibition of DPPH} = [\text{Absorbance of control} - \text{Absorbance of sample} / \text{Absorbance of control}] \times 100$$

2.5 Cell Viability Assay

The cytotoxicity of ZnHANPs was evaluated using the MTT assay. MCF-7 cells were exposed to different concentrations of ZnHANPs (20–100 mg/mL) for a whole day. After filling each well with 100 mg/mL of MTT solution, the plates were incubated at 37°C for four hours. The formed formazan crystals were dissolved in dimethyl sulfoxide (DMSO) following the removal of the growing medium. The optical density at 540 nm was measured using a microplate reader to evaluate the cells' viability. A previously reported approach was used to calculate the percentage of cell survival [15].

2.6 AO/EtBr Staining Assay

The study used the acridine orange/ethidium bromide staining technique to treat MCF-7 cells. A 100 mg/mL dye mixture was added to a 1×10^5 cell solution, which was then isolated, washed with PBS, and stained with one millilitre of the stain. A 400x magnification fluorescent microscope and an excitation filter set to 480 nm were then used to study the cells.

2.7 DAPI Staining Assay

The previously described treatment was administered to MCF-7 cells for about 48 hours following their exposure to ZnHANPs nanoparticles for DAPI nuclear labelling. The cells were then immobilised using a

^{6*}Corresponding Author Mail id: jaicitra@yahoo.co.in

solution that included methanol and acetic acid in a volumetric ratio of one to three. Following immobilisation, we washed the cells with a concentrated PBS solution. After cleaning the cells, we treated them further using a solution containing 1 mg/mL of DAPI. For twenty minutes after that, we kept this treatment out of the light. We were able to acquire pictures of the stained materials by using a fluorescence microscope and the proper excitation filter.

3. Results and Discussions

3.1 X-ray Diffraction Outline

Characteristic peaks at 2θ values of 50° , 45° , 39° , 32° , and 29° were seen in the synthesised ZnHANPs' XRD pattern, with the strongest peak occurring at 30.1° (Fig.1). The significant peak at 31.8° in this diffraction profile was quite similar to that of ordinary hydroxyapatite. The ZnHANPs' average crystallite size, as determined by Scherrer equation analysis, was 55 nm, which is within the normal range of 50-90 nm for hydroxyapatite [17]. Because of their identical crystallite sizes, the green-synthesized ZnHANPs appear to have structural features that are similar to those of conventional hydroxyapatite, which makes them attractive options for applications that call for hydroxyapatite-like qualities. It is commonly known that the size of crystallites has a major impact on the characteristics and processability of bioceramic materials.

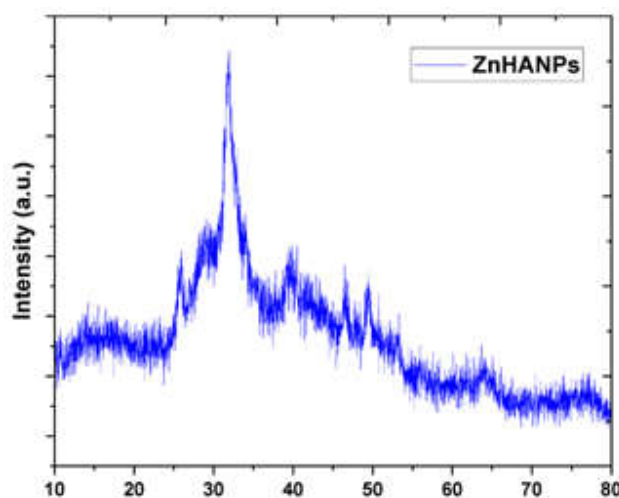


Figure 1 XRD pattern of ZnHAP nanoparticles using spinach extract as a green template

3.2 FT-IR Spectra

FT-IR spectroscopy was utilised to characterise the synthesis and structure of ZnHANPs. As observed in Figure 2, the spectra had distinct peaks at 3422 , 1053 , 612 , and 555 cm^{-1} . The strong band at 3431 cm^{-1} is caused by the stretching vibration of the hydroxyl (O-H) group, which is a characteristic feature of compounds containing hydroxyls [18]. This observation implies that the ZnHANP structure has been modified to include hydroxyl groups. The presence of absorption bands at 555 , 612 , and 1053 cm^{-1}

*Corresponding Author Mail id: jaicitra@yahoo.co.in

provides strong evidence for the efficient synthesis of ZnHANPs. Specifically, the peaks at 612 and 555 cm^{-1} indicate the bending vibrations of the O-P-O link in the phosphate group (PO_4^{3-}) [19]. The FT-IR data shown here support the formation and structural features of the synthesised ZnHANPs and are in agreement with those reported by Ravi et al. [20].

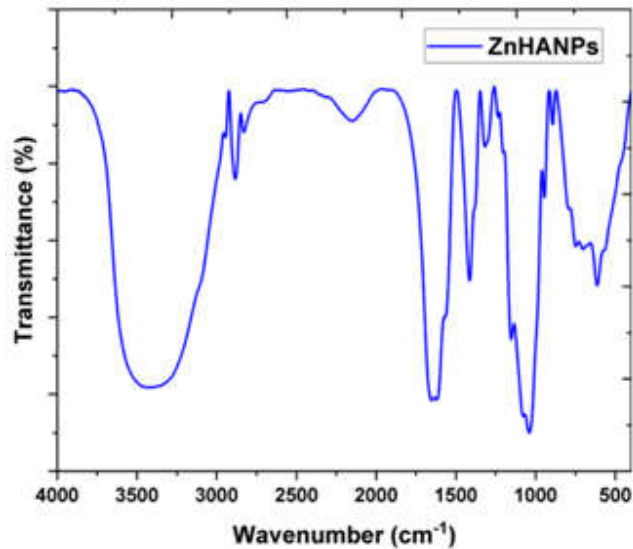


Figure 2 FTIR spectrum of ZnHAP nanoparticles using spinach extract as a green template

3.3 SEM analysis

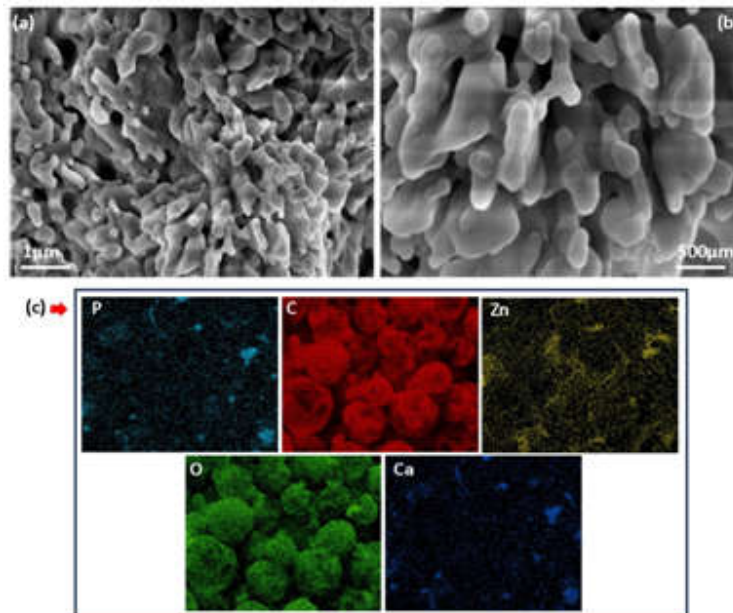


Figure 3 (a-b) Field Emission Scanning Electron Microscopy (FE-SEM) images of ZnHANPs and (c) Elemental mapping images of ZnHANPs

*Corresponding Author Mail id: jaicitra@yahoo.co.in

Figure 2a-b displays the synthesised ZnHANPs' FE-SEM picture, which mostly displays rod nanoparticles. Similar rod-like HAP structures have been shown to exist in earlier studies [21, 22]. Studies such as those conducted by Ofudje et al. suggest that HA may form rod-like structures [23]. Because of their distinctive design, these rod-shaped HAP nanoparticles could be more advantageous than conventional spherical HAP nanoparticles. HAP promotes bone growth and repair because its rod-shaped form closely resembles the natural structure of bone. The geometry of the rods could allow for precise medication delivery to particular tissues or cells. The ZnHANPs' elemental mapping picture, as seen in Fig. 2c, verified that the elements calcium (Ca), zinc (Zn), phosphorous (P), and oxygen (O) were present. The presence of discernible peaks in the intensities of these components confirms the ZnHA composition of the produced material.

3.5 Antioxidant activity

The antioxidant ability of ZnHANPs was assessed using the DPPH assay (Figure 4). The results demonstrated a concentration-dependent increase in free radical scavenging activity. While the lowest dosage had very little inhibitory impact, higher dosages demonstrated a noticeable antioxidant potential. These findings are in line with previous studies that reported on the antioxidant properties of similar materials [25, 26]. The antioxidant activity of ZnHANPs appears to be comparable to that of well-known natural antioxidants. Neutralising reactive oxygen species (ROS), which are hazardous substances that can harm cells and tissues, is the basic procedure. ZnHANPs effectively quench ROS to minimise oxidative stress. According to the DPPH assay, ZnHANPs' antioxidant activity often rose in a concentration-dependent fashion, which is consistent with the behaviour of other naturally occurring antioxidants. Its ability to scavenge free radicals suggests potential use in reducing oxidative stress.

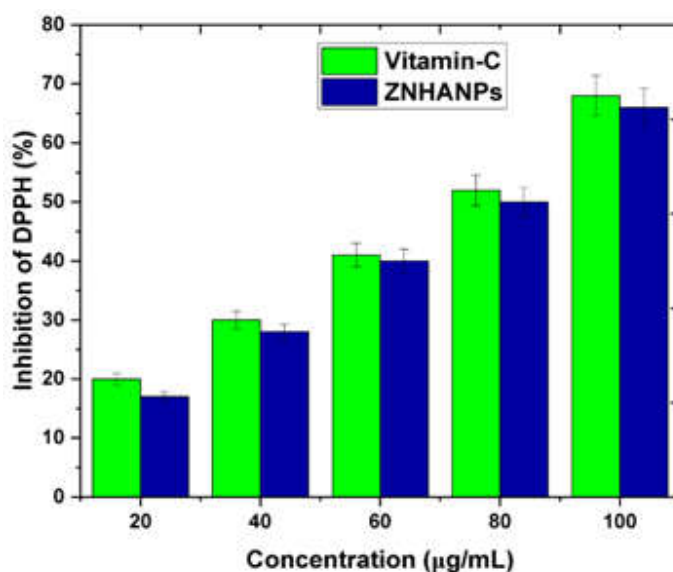


Figure 4 The antioxidant capacity of the synthesized ZnHANPs as determined by the DPPH assay

*Corresponding Author Mail id: jaicitra@yahoo.co.in

3.6 Antibacterial activity

Osteomyelitis is a debilitating disease characterised by inflammation of the bones and potential tissue damage that often requires long-term antibiotic therapy [27]. When treating bacteria that are resistant to antibiotics, this type of treatment might lead to adverse effects and treatment failures. ZnHANPs shown strong antibacterial activity against both Gram-positive and Gram-negative bacteria. The inhibitory effect was concentration-dependent and more efficient against Gram-positive *Bacillus subtilis* (zone of inhibition: 15 ± 0.28 mm) than Gram-negative *Escherichia coli* (zone of inhibition: 12 ± 0.74 mm).

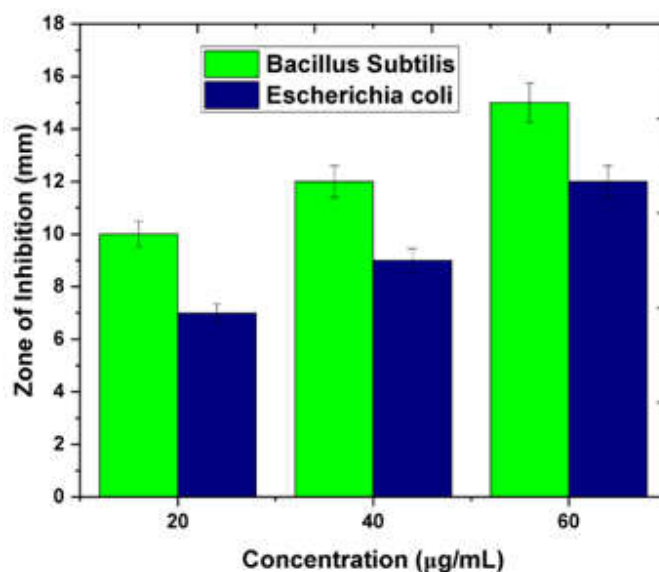


Figure 5 Antibacterial activity of synthesized ZnHANPs at different doses

3.7 MTT assay

In order to understand how tumour cells respond to harmful substances, the MTT test at 620 nm employing calorimetry was used to assess the vitality of breast cancer cells. Green-synthesised ZnHANPs reduced MCF-7 cell viability by 46 mg/mL (IC₅₀) and violet fluorescence was seen in living cells because of the presence of cellular NADPH in DNA. When ZnHANP concentration increases, this drop in colour intensity indicates a decline in cancer cell survival. The MTT test was used to evaluate quercetin NPs' effects on MCF-7 cells. Zarban et al. found that spherical ZnHANPs from *Artocarpus gomezianus* fruit decreased MCF-7 cell growth, contingent on dose [28]. The morphology of the MCF-7 cells was examined using phase-contrast microscopy, which showed unevenness, shearing, and aggregation. Additionally, these cells showed compressed nuclei and chromatin in contrast to the control cells (Figure 6b). Metal oxide nanoparticles (NPs) and their peptide conjugates inhibit endothelial cell proliferation via interacting with mitochondria, vascular promoters, and endothelial growth factors.

*Corresponding Author Mail id: jaicitra@yahoo.co.in

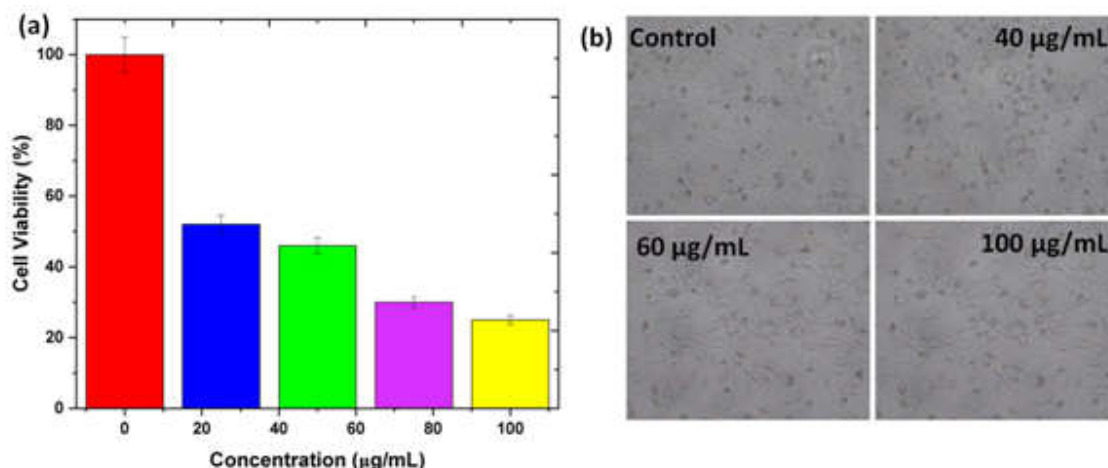


Figure 6 The anticancer effects of ZnHANPs on MCF-7 cells. Panel (a) presents MTT assay results confirming the inhibitory effect of ZnHANPs on cell viability. Panel (b) displays microscopic images illustrating morphological changes in MCF-7 cells exposed to various ZnHANP concentrations

3.9 DAPI staining assay

To ascertain whether apoptotic cells were present, DAPI labelling was used to examine the malignant cell nucleus's death. After being exposed to ZnHANPs at different doses for 24 hours, the MCF-7 cells displayed nucleus disintegration and an apoptotic tendency, in contrast to the reference cell (Figure 7). Cells going through apoptosis were easier to see because to DAPI labelling. This method uses DAPI to bind to damaged DNA and emit a vivid blue light that is especially absorbed by live cells.

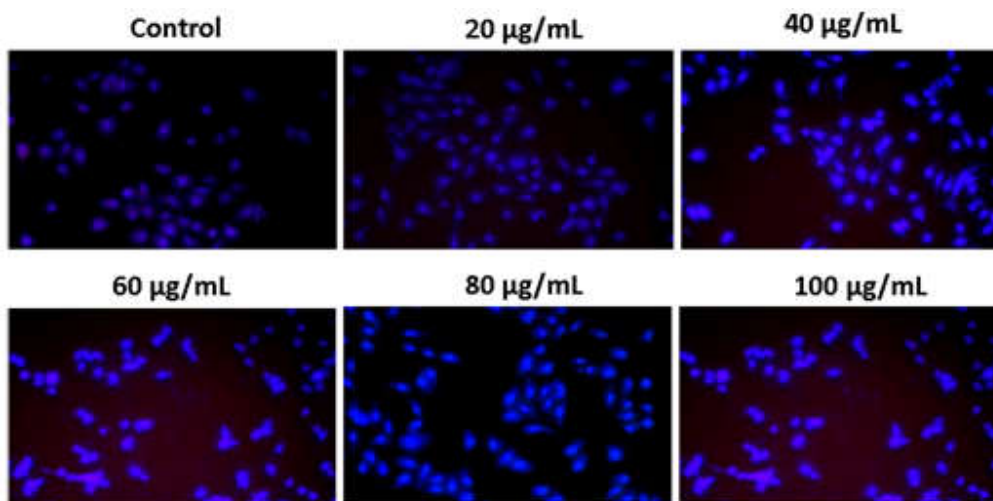


Figure 7 Morphological changes in MCF-7 cells after 24 hours of ZnHANP treatment, as observed under DAPI fluorescence staining

Bharathi and her colleagues postulated that DAPI labelling effectively activated dead cells when they were exposed to a CS/Ag nanocomposite loaded with kaempferol during incubation [30]. Therefore,

*Corresponding Author Mail id: jaicitra@yahoo.co.in

based on the staining techniques that have already been investigated, it has been hypothesised that ZnHANPs may induce apoptosis via generating ROS in cancer cells.

4. Conclusion

The study provides an economical and environmentally responsible method for producing biogenic ZnHANPs using aqueous leaf extract from *Spinacia oleracea* L. The resulting nanoparticles have the form of nanorods and are pure and crystalline. The toxicity of ZnHANPs nanoparticles was assessed using the MTT test, morphological analysis, and fluorescent labelling. The findings showed that ZnHANPs nanoparticles were effective in making breast cancer cells poisonous, which stopped them from proliferating and led to programmed cell death. These nanoparticles demonstrate that ZnHANPs nanoparticles may be made in an environmentally friendly way, which makes them attractive options for in vivo therapies. The study aims to examine the unique anti-breast cancer properties of these nanoparticles in a laboratory setting in order to use this innovative approach for industrial and therapeutic applications.

References

1. Anand U, Jacobo-Herrera N, Altemimi A, Lakhssassi N., *Metabolites*. 2019 Nov 1;9(11):258.
2. Chaachouay N, Zidane L, 2024 Feb 19;3(1):184-207.
3. Szczyglewska P, Feliczak-Guzik A, Nowak I., 2023 Jun 22;28(13):4932.
4. Zhang K, Zhou Y, Xiao C, Zhao W, Wu H, Tang J, Li Z, Yu S, Li X, Min L, Yu Z., *Science advances*. 2019 Aug 2;5(8):eaax6946.
5. Gu M, Li W, Jiang L, Li X., *Acta Biomaterialia*. 2022 Aug 1;148:22-43.
6. Devan and Venkatasubbu G, Ramasamy S, Ramakrishnan V, Kumar J., *3 Biotech*. 2011 Oct;1:173-86.
7. Verma J, Warsame C, Seenivasagam RK, Katiyar NK, Aleem E, Goel S., 2023 Sep;42(3):601-27.
8. Wu P, Han J, Gong Y, Liu C, Yu H, Xie N., *Pharmaceutics*. 2022 Sep 21;14(10):1990.
9. Roberts JL, Moreau R. Functional properties of spinach (*Spinacia oleracea* L.) phytochemicals and bioactives. *Food & function*. 2016;7(8):3337-53.
10. Caparrotta S, Masi E, Atzori G, Diamanti I, Azzarello E, Mancuso S, Pandolfi C., *Scientia Horticulturae*. 2019 Oct 15;256:108540.
11. Oruma YU, Abraham OJ, Odiba PA, Egwemi IO, Okwutachi AM, Aye GA, Yahaya A., *Dutse J Pure Appl Sci*. 2021;7:134-42.
12. Kureshi AA, Ghoshal S, Adsare S, Saste G, Mirgal A, Girme A, Hingorani L., *ACS Food Science & Technology*. 2023 Feb 2;3(2):273-82.
13. Salehi B, Tumer TB, Ozleyen A, Peron G, Dall'Acqua S, Rajkovic J, Naz R, Nosheen A, Mudau FN, Labanca F, Milella L., *Trends in Food Science & Technology*. 2019 Jun 1;88:260-73.

*Corresponding Author Mail id: jaicitra@yahoo.co.in

14. Milardovic S, Iveković D, Rumenjak V, Grabarić BS., *Electroanalysis: An International Journal Devoted to Fundamental and Practical Aspects of Electroanalysis*. 2005 Oct;17(20):1847-53.
15. Stockert JC, Blázquez-Castro A, Cañete M, Horobin RW, Villanueva Á., *Acta histochemica*. 2012 Dec 1;114(8):785-96.
16. Rabiei M, Palevicius A, Monshi A, Nasiri S, Vilkauskas A, Janusas G., *Nanomaterials*. 2020 Aug 19;10(9):1627.
17. Mehta D, Saharan VK, George S., *Environmental Science and Pollution Research*. 2023 Apr 11:1-3.
18. Rintoul L, Wentrup-Byrne E, Suzuki S, Grøndahl L., *Journal of Materials Science: Materials in Medicine*. 2007 Sep;18:1701-9.
19. Itua AN, Oluwole OI, Rangappa SM, Siengchin S., *Journal of Chemical Technology and Metallurgy*. 2023 Jan 31;58(6):1080-92.
20. Ravi ND, Balu R, Sampath Kumar TS., *Journal of the American Ceramic Society*. 2012 Sep;95(9):2700-8.
21. Latocha J, Wojasiński M, Janowska O, Chojnacka U, Gierlotka S, Ciach T, Sobieszuk P., *AIChE Journal*. 2022 Dec;68(12):e17897.
22. Ali AF, Alrowaili ZA, El-Giar EM, Ahmed MM, El-Kady AM., *Ceramics International*. 2021 Feb 1;47(3):3928-37.
23. Ofudje EA, Adedapo AE, Oladeji OB, Sodiya EF, Ibadin FH, Zhang D., *Journal of Environmental Chemical Engineering*. 2021 Oct 1;9(5):105931.
24. Nathanael AJ, Im YM, Oh TH., *Advanced Powder Technology*. 2020 Jan 1;31(1):234-40.
25. Asghar MS, Ghazanfar U, Idrees M, Irshad MS, Haq Z, Javed MQ, Hassan SZ, Rizwan M., *Kuwait Journal of Science*. 2023 Apr 1;50(2):97-104.
26. Kumar R, Shikha D, Sinha SK., *Ceramics International*. 2024 Apr 15;50(8):13967-73.
27. Urish KL, Cassat JE. *Staphylococcus aureus osteomyelitis: bone, bugs, and surgery*. *Infection and immunity*. 2020 Jun 22;88(7):10-128.
28. Zarban A, Azaryan E, Binabaj MM, Karbasi S, Naseri M., *BMC Complementary Medicine and Therapies*. 2023 Sep 26;23(1):338.
29. Ghate P, Prabhu D, Murugesan G, Goveas LC, Varadavenkatesan T, Vinayagam R, Chi NT, Pugazhendhi A, Selvaraj R., *Environmental Research*. 2022 Nov 1;214:113917.
30. Bharathi D, Ranjithkumar R, Nandagopal JG, Djearamane S, Lee J, Wong LS., *Environmental Research*. 2023 Dec 1;238:117109.

^{6*}Corresponding Author Mail id: jaicitra@yahoo.co.in